Low-Loss RF Transport Over Long Distances

M. Friedman and Richard F. Fernsler

***Abstract*—Electromagnetic RF energy can be transported over a kilometer or more using antennas, but the efficiency is low unless the injecting and receiving antennas are extremely large. Other means of transporting RF energy such as waveguides and coaxial lines are cumbersome, heavy, costly, and suffer large attenuation. This paper offers a different system for long-distance RF transportation. The key is to use nonradiating electromagnetic surface waves that propagate along thin metallic strips. This means of moving RF energy between two points is simple, inexpensive, lightweight, and has low attenuation. For example, the attenuation is less than 2 dB/km for an Al foil 6-cm wide and 0.002-cm thick. Thus, efficient guidance of surface waves over distances of many kilometers requires neither large antennas, waveguides, nor coaxial lines. Moreover, electric interference with the surroundings is minimized due to the large reduction in the radial extension of the electric field, and the conversion of the radiating electromagnetic waves to surface waves and back is efficient (up to 90%).**

***Index Terms*—High-power microwaves, RF transport, surface waves.**

I. Introduction

THE standard way of transporting RF energy is to inject it into free space through an antenna and then receive it with a second antenna. As is well known [1], the RF power P_s radiated through an antenna of area A_s is related to the power P_t received by an another antenna with area A_t by

$$\frac{P_s}{P_t} = \frac{\lambda^2 R^2}{A_s A_t} \tag{1}$$

where λ is the RF wavelength and R is the distance between the two antennas. The transfer ratio P_s/P_t reaches unity, for example, for $\lambda = 0.3$ m and $R = 1$ km, if $A_s = A_t = 300$ m^2. With these parameters, one can get the theoretical maximum efficiency for RF energy transportation. However, for longer distances or longer wavelength, the efficiency becomes small unless both antennas are very large.

Another means of transporting RF or microwave energy is to use enclosed transmission lines such as hollow waveguides or coaxial lines. However, this technique is practical only over short distances. For propagation over long distances, waveguides and coaxial lines are too cumbersome, heavy, and lossy. For example, electromagnetic energy at a frequency of 1 GHz can be transported using an L-band waveguide made out of Al, but the weight exceeds 10 t/km and the attenuation exceeds 10 dB/km [2]. The attenuation is even worse for coaxial lines such as RG19A/U. Here, the weight is only 1.1 t/km, but the attenuation is 150 dB/km.

There are other type of transmission lines in which the electromagnetic energy is not confined by conducting walls [2]–[7], but flows outside the structure in free space. In such systems, the electric field of the wave extends radially far outside the structure, and most of the energy is confined within a few wavelengths around the structure. Such transmission lines are light, have low attenuation, and are inexpensive. Examples of such structures are metallic wires with [4] or without dielectric cover [3], metallic plates with dielectric cover [8], and corrugated guides [7]. The electromagnetic waves (named surface waves) propagate on these guides with a phase velocity $< c$. Their properties are governed by the surface impedance $Z = E_T/H_T$, where E_T and H_T are the tangential components of the electric and magnetic fields. These waves are nonradiating and may exist simultaneously, in the same structure with radiating waves. Electromagnetic waves (radiating or surface waves) have electric (E) and magnetic (B) fields that satisfy Maxwell equations

$$\nabla \times E = -\frac{\mathrm{dB}}{dt} \quad \nabla \times B = \sigma\,\mu E + \mu\varepsilon \frac{dE}{dt}. \tag{2}$$

Here, σ is the conductivity, ε is the permittivity, and μ is the permeability of the medium.

Sommerfeld was the first to theoretically investigate nonradiating electromagnetic waves that propagate on a metallic wire of circular cross section and of finite conductivity [3]. He found that the most important mode is axisymmetric and transverse magnetic. For this mode, the radial electric field can be expressed outside the wire in the form

$$\begin{aligned} E_r &= AK_1(ur)\exp(i\omega t - hx), \qquad h = a + i\beta \\ \beta &= \frac{2\pi}{\lambda} = \frac{\omega}{c}. \end{aligned} \tag{3}$$

Here, x measures distance along the wire, r measures distance from the wire center, A is a constant related to the wave power, ω is the angular wave frequency, K_1 is the first Hankel function of order one, h is the complex propagation coefficient, and u is the complex radial decay coefficient. The latter is related to the propagation coefficient by

$$u = a - ib = \sqrt{\beta^2 - h^2}. \tag{4}$$

At small distances from the wire, $K_1(ur)$ behaves like $1/r$, but at large distances, $K_1(ur)$ varies as $\exp(-ur)(\pi/2ur)^{1/2}$. Sommerfeld showed that the transverse electromagnetic field is continuous across the wire boundary, and then he determined u by calculating the surface impedance in the metal Z_m and the

Manuscript received September 21, 1999. This work was supported by the Navy Engineering Logistics Office.

The authors are with the Plasma Physics Division, Naval Research Laboratory, Washington, DC 20375 USA.

Publisher Item Identifier S 0018-9480(01)01075-4.

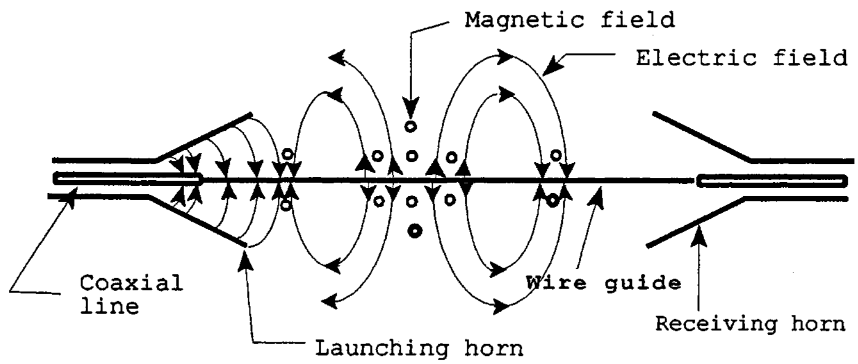

Fig. 1. Launching surface waves on wires and receiving them using coaxial horns [5].

surface impedance in air (or vacuum) Z_a and equating them at the radius ρ of the wire

$$Z_m = \frac{J_0(u\rho)}{J_1(u\rho)} \left[\frac{u}{\sigma + i\omega\varepsilon_m}\right] \quad Z_a = \frac{K_0(u\rho)}{K_1(u\rho)} \left[\frac{u}{i\omega\varepsilon_0}\right]. \quad (5)$$

Here, K_0 is a Hankel function of order 0, J_0 and J_1 are Bessel functions of order 0 and 1. Sommerfeld thereby obtained the solution $u \approx (0.2 - 0.1\ i)$ Np/m for a Cu wire 1 mm in radius carrying a surface wave with a frequency of 1 GHz. The axial attenuation, which is proportional to the skin depth divided by the wire radius, is small in this case: $\alpha \approx 0.0014$ Np/m ($= 0.012$ dB/m). Moreover, 99% of the wave energy is confined within a distance of 6 m from the wire. The axial and radial decay attenuation coefficients are interdependent, i.e., $\alpha = (c/\omega)\ (ab)$, and both coefficients increase with frequency and decrease with wire size. For large diameter wires, the radial decay coefficient is so small that the wave is barely attached to the conductor. For example, for $\rho \rightarrow \infty$, the wire is equivalent to an infinitely wide plane [5]. In this limit, $\alpha = 2\pi^2/(\sigma Z_0 \lambda^2) \approx 5 \times 10^{-8}$ Np/m, where $Z_0 = 377\,\Omega$ and $u = (1-i)(2\pi/\lambda)^{3/2}(1/2\sigma Z_0) \approx (1-i)10^{-3}$ Np/m. The axial decay is, therefore, negligible, but the electric field of the wave extends radially to over 100 m from the conductor surface. This is the reason why a bare small diameter Cu wire is a practicable waveguide for surface waves, while a bare flat Cu sheet is not. Even so, surface waves on a bare wire extend sufficiently far radially that they can suffer large losses due to scattering from nearby objects. Also, small bends and sags on the wire severely attenuate the waves.

Goubau [4] and others [5] suggested that coating the guiding structures with dielectric and/or inserting corrugation increases the surface reactance, thus reducing the radial extension of the electric field and allowing the wave to propagate around corners [4], [5].

For example, covering a metal sheet with a dielectric layer of thickness $\boldsymbol{l}$ and permittivity ε increases the complex radial coefficient to $u = (1-i)(2\pi/\lambda)^{3/2}(1/2\sigma Z_0) + (2\pi/\lambda)^2 \boldsymbol{l}(\varepsilon - \varepsilon_0)/\varepsilon_0$. The real part of u is then large even for small $\boldsymbol{l}$. Note that the electric-field compression is accompanied by an increase in axial attenuation. Similar results apply to wires. An example [9] is a Cu wire of 1.42-cm diameter with a polyethylene coating 0.34-cm thick. This wire had an attenuation of 2.5 dB/km at a frequency of 300 MHz and a weight of 2 t/km.

The guidance of surface waves around bends strongly depends on the value of the radial decay coefficient a. For example, calculations [5] showed that waves on a wire would follow a bend with a radius of curvature $R > R_0 = (2\pi)^2/(2^{1/2}\lambda^2 a^3)$ without attenuation.

Surface waves on wires are typically excited on wires by connecting one end of the wire to the center conductor of a coaxial conical horn with an outer radius of the order of a few wavelengths. The horn is then energized by an RF source. The surface waves can be converted back to RF by connecting the other end of the wire to a similar horn (Fig. 1). The conversion of RF to surface wave and back to RF is a reciprocal process when the two horns are the same. The efficiency of launching a surface wave can exceed 90%.

In this paper, we revisit the propagation of surface waves. We will show in Section II that a lightweight conductor in the shape of a metallic strip a few skin depths thick and less than a half-wavelength wide can transmit surface waves efficiently and economically over long distances. In Section III, we present experimental results for surface waves propagating on metallic strips. In Section IV, we show how surface waves can be converted to electromagnetic waves (and vice versa) using a system of two rectangular waveguides with transverse dimensions equal to $\lambda/2$.

II. Theory of Surface-Wave Propagation on Metallic Strips

To solve Maxwell's equations for a strip, we use elliptic coordinates $(x,\ \xi,\ \eta)$. These are related to Cartesian coordinates by the equations $x = x$, $y = q\cosh\zeta\cos\eta$, $z = q\sinh\zeta\sin\eta$, where x is the propagation direction along the strip. Half the distance between the foci is q, which is approximately equal to the half-width of the strip. The foil surface coincides with the ellipse $\zeta = \zeta_0$ where, e.g., $\zeta_0 = 0.0003$ for a foil with $q = 3$ cm and thickness $2\delta = 0.002$ cm (see Fig. 2).

It is assumed that the wave has electric-field components $(E_x,\ E_\zeta,\ 0)$ and magnetic-field components $(0,\ H_\eta,\ 0)$ that vary as $\exp(i\omega t - hx)$. Maxwell's equations can then be written as

$$(\sigma + j\omega\varepsilon) q_1^2 E_x = \frac{\partial (q_1 H_\zeta)}{\partial \eta}$$

$$(k^2 + h^2) q_1 E_\zeta = -\,h \frac{\partial E_x}{\partial \zeta}$$

$$-(k^2 + h^2) q_1 H_\eta = (\sigma + i\omega\varepsilon) \frac{\partial E_x}{\partial \zeta} \quad (6)$$

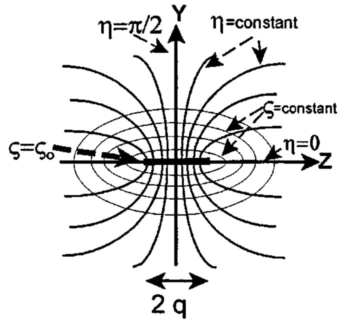

Fig. 2. Elliptic coordinate system. $\zeta = \zeta_0 = 0.003$ is the coordinate of the surface of the strip and $2q$ is the strip width.

where $h = \alpha + i\beta$ is the complex propagation constant, $q_1 = q(\sinh^2\zeta + \sin^2\eta)^{1/2}$, and $k^2 = \omega^2\varepsilon\,\mu - i\omega\,\mu\sigma$. All the components of the fields are in terms of E_x, and the wave equation for E_x is [10]

$$\left[\frac{\partial^2}{\partial\zeta^2} + \frac{\partial^2}{\partial\eta^2} + (k^2+h^2)q^2(\sinh^2\zeta + \sin^2\eta)\right]E_x = 0. \tag{7}$$

Note that $\mathrm{Real}(k^2 + h^2) < 0$, which corresponds to slow waves. After separating variables, (7) reduces to radial and angular Mathieu equations with solutions of order $n = 0, 1, 2, 3, \cdots$ The solution of the wave equation is $E_x = \sum W_n Se_n(\eta)\mathrm{Re}_n(\zeta)$, where $Se_n(\eta)$ and $\mathrm{Re}_n(\zeta)$ are the nth-order angular and radial Mathieu functions. Here, W_n are constants related to the power of the different modes propagating on the strip. From (6), one can show that the transverse magnetic field H_η and the perpendicular electric field E_ζ in elliptical coordinates are given by

$$\begin{aligned} H_\eta &= -\frac{(\sigma + i\omega\varepsilon)}{(k^2+h^2)q(\sinh^2\zeta + \sin^2\eta)^{1/2}}\,\frac{\partial E_x}{\partial\zeta} \\ E_\zeta &= \left[\frac{h}{\sigma + i\omega\varepsilon}\right]H_\eta. \end{aligned} \tag{8}$$

Precise calculations to determine the modes at large x are cumbersome; instead, we note that different modes attenuate along x at different rates, depending on the electromagnetic-wave penetration into the foil. Modes that penetrate little into the foil (decay rapidly with ζ inside the foil) suffer relatively little ohmic loss and thus attenuate slowly. Hence, the dominant modes at large x inside the foil are usually those with large $\partial/\partial\zeta$ and, therefore, small $\partial/\partial\eta$ [see(7)]. Thus, we shall concentrate on modes with $\partial/\partial\eta \to 0$, which correspond to the axisymmetric modes studied by Sommerfeld [3].

Outside the foil where $\sigma = 0$, propogating modes with wavelength larger than the foil width and with low attenuation have a dimensional scale parameter $|k^2 + h^2|q^2 \ll 1$. In this limit, the only mode with $\partial/\partial\eta \to 0$ is $Se_0(\eta)$. Consequently, we need to consider only $Se_0(\eta)$ and $\mathrm{Re}_0(\zeta)$ to examine long-wavelength modes outside the foil. For use later, we express the radial function as a sum of Hankel functions [11]

$$\begin{aligned} \mathrm{Re}_o(\zeta) &= B\sum_0^\infty A_{2n}Q^nK_{2n}\left(2\sqrt{Q}\cosh\zeta\right) \\ &\approx B\left[K_0(2\sqrt{Q}\cosh\zeta) + \frac{Q}{2}K_2\left(2\sqrt{Q}\cosh\zeta\right)\right. \\ &\qquad \left. + \frac{Q^2}{32}K_4\left(2\sqrt{Q}\cosh\zeta\right) + \cdots\right]. \end{aligned} \tag{9}$$

where

$$\begin{aligned} Q &= -(k^2+h^2)q^2/4 \\ B &= \text{constant} \\ A_0 &= 1 \\ A_{2n} &= \frac{2}{(n!)^2}\left[\frac{1}{4}\right]^n, \qquad \text{for } n \succeq 1\ Q \to 0 \end{aligned}$$

The wave impedance is given by the ratio E_x/H_η at the foil surface. To compute the impedance Z_a in air, we take $|Q| \ll 1$ and $\cosh\zeta_0 \approx 1$. We then obtain the following approximate relationships (for $n > 0$):

$$\begin{aligned} &Q^nK_{2n}(2Q^{1/2}\cosh\zeta_0) \\ &\quad\approx (2n-1)!/\left\{2(\cosh\zeta_0)^{2n}\right\} \approx (2n-1)! \\ &\left[\partial\left(K_0(2Q^{1/2}\cosh\zeta)\right)\Big/\partial\zeta\right]_{\zeta=\zeta 0} \\ &\quad= -2Q^{1/2}\sinh\zeta_0\left[K_1(2Q^{1/2}\cosh\zeta)\right]_{\zeta=\zeta 0} \\ &\quad\approx -\sinh\zeta_0/\cosh\zeta_0 \\ &Q^n\left[\partial\left(K_{2n}(2Q^{1/2}\cosh\zeta)\right)\Big/\partial\zeta\right]_{\zeta=\zeta 0} \\ &\quad\approx -\sinh\zeta_0(2n)!/\left\{2(\cosh\zeta_0)^{2n+1}\right\} \\ &\quad\approx -2Q^{1/2}\sinh\zeta_0\left[K_1(2Q^{1/2}\cosh\zeta\right]_{\zeta=\zeta 0}(2n)!\Big/ \\ &\qquad\left\{2(\cosh\zeta_0)^{2n}\right\}. \end{aligned}$$

Substituting these approximations into (9), we calculate the surface impedance Z_a at $\zeta = \zeta_0 = 0.0003$ using (8)

$$\begin{aligned} Z_a &\approx i\frac{\left[-(k^2+h^2)\right]^{1/2}}{\omega\varepsilon_0}\,\frac{\left[\sinh^2\zeta_0 + \sin^2\eta\right]^{1/2}}{\sinh\zeta_0} \\ &\qquad\cdot\frac{K_0\left(2\sqrt{Q}\right) + C_1}{K_1\left(2\sqrt{Q}\right)C_2} \\ C_1 &= \sum A_{2n}\frac{(2n-1)!/2}{\cosh^{2n}\zeta_0} \approx 0.25 + 0.093 + 0.051 \\ &\qquad + 0.03 + 0.01 + O(0.01) \approx 0.45 \\ C_2 &= 1 + \sum A_{2n}\frac{(2n)!/2}{\cosh^{2n}\zeta_0} \approx 1 + 0.5 + 0.375 \\ &\qquad + 0.3125 + 0.2621 + \cdots \\ n &= 1, 2, 3, \ldots, \infty \end{aligned} \tag{10}$$

where C_1 and C_2 are positive numbers. These sums can be terminated when $\cosh^{2n}\zeta_0 \gg 1$.

A different approach must be taken to calculate Z_m inside the metal (thickness >5 skin depths). The wavenumber k', inside the foil of high-conductivity, satisfies $k'^2 = -i\omega\ \mu(\sigma + i\omega\varepsilon) \approx -i\omega\ \mu\sigma \gg h^2$ and $k'q \gg 1$. Here, we cannot simply use $Se_0(\eta)$ as before, but rather we need a large sum of angular Mathieu functions $Se_n(\eta)$ to generate a solution independent of η. Fortunately, Hankel functions of large argument and of any order converge to the same value and, hence, the radial Mathieu function (which can be written as a sum of Hankel functions) can be approximated by $\mathrm{Re}_n(\zeta) \approx K_n e^{-ik'q\cosh\zeta}(k'q\cosh\zeta)^{-1/2}$, where K_n are constants. In that limit, E_x inside the metal is [see also ref (10)]

$$E_x \approx F(\eta)(k'q\cosh\zeta)^{-1/2}e^{-ik'q\cosh\zeta}. \tag{11}$$

Here, $F(\eta)$ is arbitrary such that, the case of present interest is approximately equal to a constant. H_η is found from E_x using (8) and, hence, at $\zeta = \zeta_0$

$$Z_m = (1+i)\left[\frac{\omega\,\mu}{2\sigma}\right]^{1/2}\frac{\left[\sinh^2\zeta_0 + \sin^2\eta\right]^{1/2}}{\sinh\zeta_0}. \tag{12}$$

Since E_x is independent of η, it can be made continuous across the foil by a proper choice of the parameters. In that case, a sufficient and equivalent condition for H_η to be continuous across the foil boundary is to equate Z_a to Z_m, which yields the dispersion relationship

$$\begin{aligned}[1+i]\left[\frac{\omega\,\mu}{2\sigma}\right]^{1/2} &= (R+iX)\\ &\approx i\frac{2\sqrt{Q}}{q\omega\varepsilon_0}\frac{K_0(2\sqrt{Q})+C_1}{K_1(2\sqrt{Q})C_2}\end{aligned} \tag{13}$$

$$(R+iX) \approx i\frac{2\sqrt{Q'}}{q\omega\varepsilon_0}\frac{K_0(2\sqrt{Q'})}{K_1(2\sqrt{Q'})},\quad \text{where } Q' = Q/C_2. \tag{14}$$

It is easy to show that $K_0(2Q^{1/2})$ is greater than C_1 and $0.5\ \ln\ (C_2/2.5)$. In that case, (13) can be rewritten in the form reminiscent [1], [3] of a wire of radius q. For $\xi = \xi_0 = 0.0003$, we find that $C_2 \geq 100$.

The solution of (14) can be written as $2Q'^{1/2} = q(a' - ib')$, where $a' = C_2^{1/2}a$ and $b' = C_2^{1/2}b$. The electric field around a thin foil of half-width q is thus more concentrated than the electric field around a wire of radius q, but it also attenuates more rapidly with distance.

Regardless of the shape, the attenuation of a surface wave on a straight conductor is given by $\alpha \approx (c/\omega)ab$. At a frequency of 1 GHz, the attenuation is $\alpha < 0.1$ dB/km for surface waves on an aluminum wire of diameter $2r = 6$ cm, whereas on a smooth aluminum strip of the same surface area as the wire (i.e., 9-cm wide and 0.002-cm thick), the wave is attenuated by <7 dB/km. However, the radial extension of E_ζ around the foil is reduced by nearly ten over the wire, thereby decreasing the scattering losses from nearby objects.

The increase in the value of the radial decay coefficient a' is even more beneficial if the foil is bent. We pointed out earlier that waves on a wire would follow a bend with a radius of curvature $R \gg R_0 = (2\pi)^2/(2^{1/2}\lambda^2 a^3)$ without attenuation. Replacing a by a' reduces R_0 by three orders of magnitude and, thus, reduces the sensitivity of surface waves to bends.

The increase in the radial decay coefficient for a foil can be understood as follows. A foil covers much less volume than a wire of the same surface area and, therefore, the field energy is more heavily concentrated around a foil. Thus, the field must fall off faster outside a foil than a wire for a given wave energy. Associated with the reduction in conductor volume is a reduction in mass, especially since a foil, unlike a wire, can be thin without collapsing. Indeed, a thin foil is almost certainly the lightest structure (weight of the order of 1 kg/km) that can be used to guide and confine RF radiation. As discussed below, a foil can be configured to reduce the axial attenuation and, as a result, *the field attenuation and mass of a thin metallic strip can be orders of magnitude smaller than a coaxial line (e.g., RG19A/U) or a waveguide of similar length.*

The surface reactance and concentration of an electric field around a foil can be enhanced by adding dielectric coating or inserting periodic discontinuities on its surface. The dielectric coating needed to make a substantial difference in the field distribution has to be many skin depths of the metal [4], which increases the weight and cost markedly. Alternatively, increased reactance can be obtained by cutting holes periodically in the middle of the foil. Other modes with $n \neq 0$ that may be excited due to the presence of the holes attenuate rapidly [2]. The periodic holes act as a one-dimensional equally spaced array of parallel short dipoles. The electric field generated by the array is equal to $E = f \times S(\theta)$, where f is the electric-field pattern determined by a single element (slot) and $S(\theta)$ is the array factor

$$S(\theta) = \sum I_n \exp(jnu), \qquad u = kp(\cos\theta - 1). \tag{15}$$

Here, θ is the direction angle with respect to x, I_n is the current amplitude in the nth slot, p is the separation between slots, and k is the wavenumber. Assuming equal I_n for all slots, $S(0) = NI_n$ in the forward direction and $S(\pi) = 0$ in the backward direction only if the number of slots in a wavelength λ/p is an integer. If λ/p is not an integer, reflection occurs.

The modified surface impedance due to the slots has an added reactance from the inductance introduced by the holes (proportional to the area of the holes). This inductance modifies X in (7), resulting in an increase in a.

III. Surface Waves on Metallic Strips—Experiment

We performed experiments to confirm the theory qualitatively. In the experiment (Fig. 3), microwave sources pumped electromagnetic energy through conical horns to different metallic conductors. In the first experiment [Fig. 3(a)], we used a low-power tunable RF continuous wave (CW) source. The center conductor of the horn was connected to the metallic conductors. The length of each conductor was 4 m. The following three different conductors were used:

1) Al tube 5 cm in diameter;
2) Al foil 6-cm wide and 0.002-cm thick;
3) same foil with rectangular holes inserted in the center at a pitch $p = 2.5$ cm.

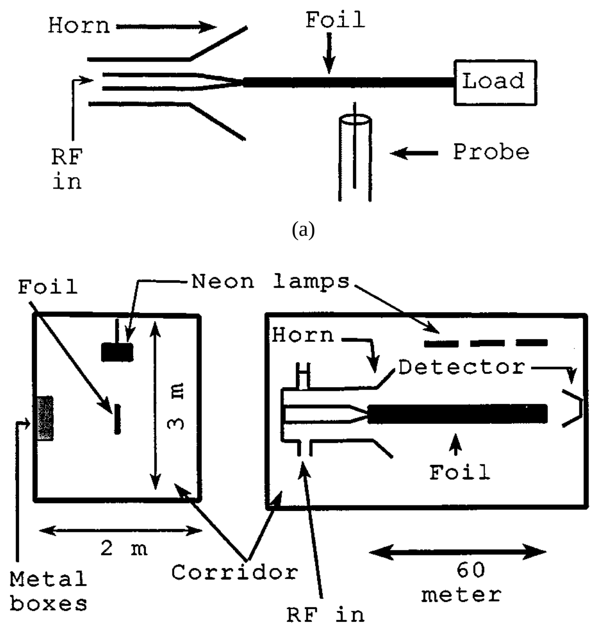

Fig. 3. Experimental arrangement for investigation of surface-wave transmission lines at: (a) low RF power and (b) high power.

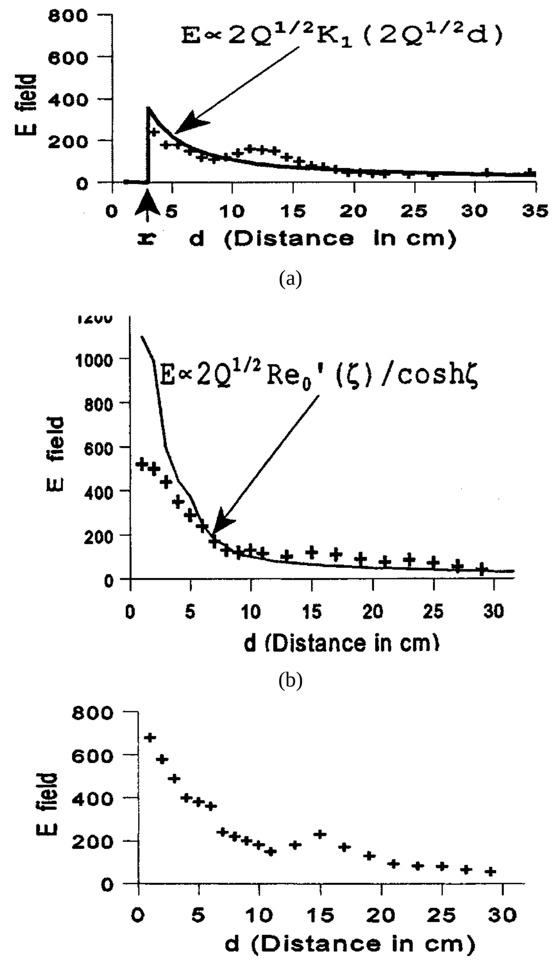

Fig. 4. Field distribution (arbitrary units) as a function of distance from the center of three different conductors. (a) Al rod 5 cm in diameter. (b) Al foil with a width of 6 cm and thickness of 0.002 cm. (c) Al foil [the same size as (b)] with rectangular holes (1 cm $\times$ 0.5 cm) placed in the center of the foil with a pitch of 2.5 cm. Theoretical curves are plotted as solid lines for (a) and the (b). In (b), $\sinh\zeta = d/q$, where $d =$ distance from the foil center. The probe was located in the case of the foils at $\eta = \pi/2$ (see Fig. 2).

The holes were 0.5-cm long, parallel to the foil, and 1-cm wide. All the conductors were terminated with a load. The foils were supported by cotton threads from the ceiling. We measured the voltage standing-wave ratio (VSWR) of the system and the RF power that emerged at the end of the conductors to ensure that the same RF power was injected and propagated as surface waves. The radial electric field was scanned using an uncalibrated probe made of a rigid 50-Ω cable with the center conductor exposed at one end. The other end was connected to an oscilloscope. The signal measured by the probe was frequency independent for the first two conductors. However, the signal transmitted by the third configuration peaked at the frequencies $f_1 = 1020$ MHz, $f_2 = 1180$ MHZ, $f_3 = 1330$ MHz, and $f_4 = 1480$ MHz. Note that $\lambda_i/p = (c/f_i p)$ is close to integers $(11.8, 10.2, 9.0, 8.1)$ as expected. At intermediate frequencies, the signal dropped, indicating large losses in the power propagated on the modified foil.

The electric-field radial distributions around the conductors were measured at 1.33 GHz. The results (Fig. 4) show that the electric field is more concentrated near the foil than near the tube. The calculated radial electric field around the wire [3] and around the foil is also shown in Fig. 3(b). The disagreement between theory and experiment is due to the probe perturbing the field. The foil with the holes had the highest electric field near the surface, showing further compression of electromagnetic energy.

In a second experiment [see Fig. 3(c)], we investigated the electromagnetic interference (EMI) of the foil transmission line on nearby objects. We injected 3 MW of RF pulses into the unmodified foil through a 1-m-diameter coaxial–conical horn. The foil was stretched in the middle of a corridor 60-m long. The corridor was 2-m wide and 3-m high. Five metallic boxes and 12 neon light fixtures were spaced, almost evenly, inside the corridor. The RF power was measured after propagating on the 60-m-long foil and was compared with the power that emerged after propagation on a 4-m-long foil. In both cases, the far end of the foil was connected to an antenna and the radiated power was measured in the atmosphere. This experiment showed that the foil attenuated the surface waves by <2 dB/km. The measured attenuation is smaller than the calculated one ($\sim$8 dB/km). The reason for the discrepancy is that the calculated attenuation coefficient α varies as C_2. For an ideal smooth foil with $\zeta_0 = 0.0003$, C_2 is a large number ($\geq$100). However, in the experiment, the foil had bends and sags that reduced the value of C_2. Good agreement between the theoretical and experimental attenuation is obtained for $C_2 \approx 20$. The low attenuation suggests that electromagnetic scattering from the metallic objects placed at a distance of three to four wavelengths was unimportant. Note that a solid Al wire of 0.4-cm radius will have a similar attenuation, but will weigh more than an order of magnitude greater.

In a third experiment to be reported in Section IV, we found that RF could be converted into surface waves and back into RF

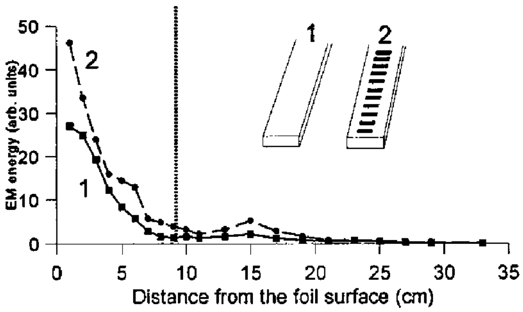

Fig. 5. Electromagnetic energy density radial distribution of surface waves that propagate on Al foil and on Al foil with periodical holes. The straight dotted line defines the narrow size of an L-band waveguide.

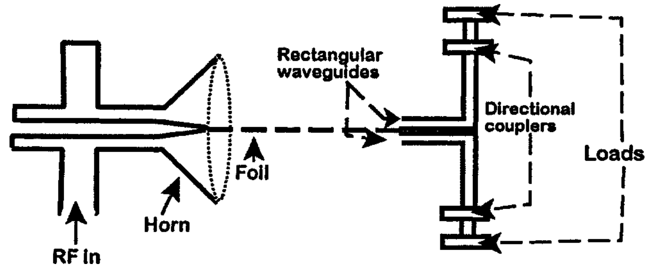

Fig. 6. Schematic arrangements showing RF conversion to surface wave and RF extraction from the surface wave into rectangular waveguides. The efficiency of transfer was calculated from the power input to the horn and from the power outputs detected by the directional couplers.

with an efficiency of almost 90%. This proves that negligible RF power leaked out from the system as radiating space waves.

The sag and small bends caused by the cotton threads that supported the foil varied during the investigation, but produced no measurable variations in the loss. Moreover, inserting a bend with a 50-cm amplitude into the 60-m-long foil did not measurably increase the attenuation. This bend had a radius of curvature $\rho \approx 1000$ m that was smaller than what theory predicts for uninterrupted propagation on wires [5]. The radius of curvature was reduced to $\rho = 200$ m using an Al foil covered by a layer of Al_2O_3 0.001-cm thick, but the attenuation remained <2 dB/km.

Propagation of surface waves on foils at lower frequencies was studied as well. Results were in accordance with the theory outlined in Section II. The lowest RF frequency that we were able to inject and convert to surface waves was around 50 MHz. Since the measured phase velocities were close to c at all frequencies, broad-band RF pulses can, in principle, be propagated over long distance with little attenuation and dispersion.

IV. Conversion of RF to Surface Waves and Back

At the strip surface ($\zeta = \zeta_0 = 0.0003$ in the examples discussed above), the electric field is perpendicular to the strip and, hence, is everywhere parallel, except at the edges. This property can be utilized to convert RF to surface waves and back.

Most of the electromagnetic energy that propagates on the strip is confined within a distance of less than a half-wavelength from the foil (Fig. 5). This distance is equal to the width of a standard waveguide (WR 770). By attaching the strip to the wide sidewall of the waveguide, nearly one-half of the electromagnetic energy enters the waveguide as RF radiation. The remaining one-half can be extracted by sandwiching the strip between another waveguide, as shown in Fig. 6. Using this configuration, we obtained 75% energy transfer from the RF source that fed the conical horn to the two waveguides when a solid strip was used, and 90% transfer when the foil with the holes was used. This result confirmed that the electromagnetic energy is compressed more tightly around foils with holes. Note that the RF in the two waveguides are 180° out of phase.

This approach can also be used to excite surface waves. RF can be injected into the two waveguides 180° out of phase. The two RF signals will combine at the waveguide–foil junction to excite a surface wave. The transverse dimensions of the two waveguides system are smaller than a wavelength and, hence, smaller than the diameter of the coaxial horns that have been used by us and others to initiate surface waves. Note that the high efficiency of conversion is due to the similar electromagnetic-field pattern around the foil and inside the waveguides.

Conversion of surface waves into radiation has been achieved before [1] using structures (antennas) at the end of transmission lines. These structures had a single (abrupt) and/or periodic discontinuities (array) in the path of the surface waves. In such systems, RF radiation has been emitted from the following three places.

- *Radiation from the junction between the guiding system and the radiating structure*. This is an undesired mode of radiation that can influence the final radiation pattern.
- *Radiation along the structure*. Here, a surface wave encounters a series of discontinuities that act as radiating elements.
- *Radiation from the end discontinuity.*

The RF that is emitted from these three regions combines to give the final radiation pattern. Only by proper choice of the RF guiding transmission line and the radiating antenna can one get the RF pattern needed.

For example, an annular radiation pattern can be achieved by using axisymmetric antennas excited by symmetrical surface waves. However, a radiation configuration with a hole in the center is generally not useful.

More useful is a RF pattern radiation that can be focused to a spot. Such a pattern can be achieved using long nonaxisymmetric antennas. However, the different boundary conditions between the fields of the surface waves and the radiating waves excite modes that attenuate rapidly [2] while propagating on wires and narrow foils, thus resulting in large energy losses.

In the present investigation, surface waves were efficiently converted to RF that could be focused to a spot. The radiating system consisted of an abrupt discontinuity in the guiding strip that was terminated by a short asymmetric antenna. In the experiment, a 4-MW microwave source pumped RF pulses with a frequency of 1.3 GHz into a coaxial, 60° conical horn with 1-m outer diameter. The horn was employed in two modes: it either radiated the RF pulses into the atmosphere or it injected the RF onto Al strips. The following two different strips were used: 1) an Al foil 6-cm wide and 0.002-cm thick and 2) a similar foil with rectangular holes that were inserted periodically along the strip in its center (see Sections II and III) The other end of

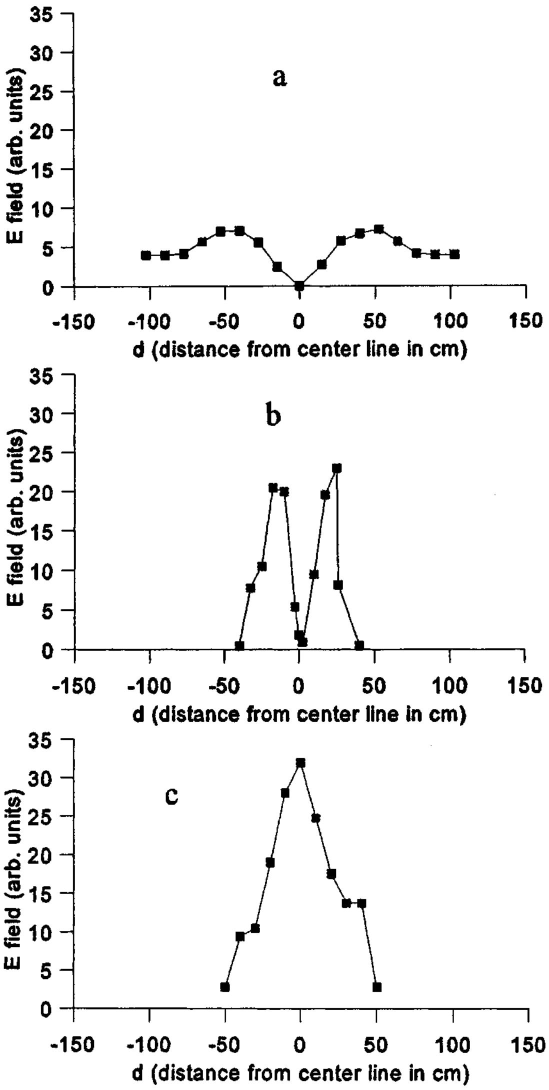

Fig. 7. (a) Radiation pattern 4.5 m away from a coaxial conical horn. (b) Pattern of RF radiation that emerged at the end of an Al foil 4-m long, 6-cm wide, and 0.002-cm thick. The radiation was measured 0.5 m away from the foil. (c) Pattern of RF radiation that emerged from the antenna (Fig. 8) that was connected to the Al foil.

the foils was connected to different radiating systems (e.g., antennas).

As expected, an annular RF pattern of radiation [see Fig. 7(a)] was observed when the RF pulses were radiated through the horn directly into the atmosphere. The power density detected at a distance L from the horn was proportional to L^{-2}.

Higher power density was obtained when the pulses were guided along the Al strip and RF radiation was emitted from the end of the foil. In that case, the final radiation efficiency was $\approx$70%. The annular radiation pattern followed the electromagnetic energy pattern of the surface waves. In this pattern, one can see the imprint of the (nearly) TEM mode characteristic of surface waves [see Fig. 7(b)]. The radiation was measured by a small antenna, and the power density received was independent of the distance L. Fig. 7(b) was taken when the RF detector was located 4.5 m from the radiating horn and 50 cm from the end of the foil.

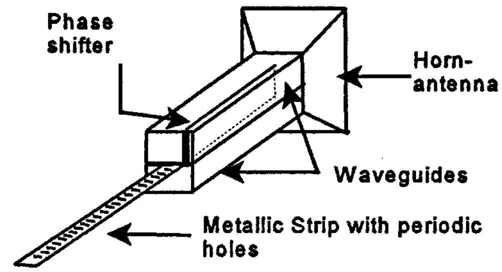

Fig. 8. RF extraction from surface waves to a TE_{01} radiation pattern [see Fig. 7(c)].

The best results were obtained when the two waveguides mentioned earlier were used. The phases of the RF waves excited in the two waveguides were 180° apart. Injecting these waves into the atmosphere from the far ends of the waveguides generated a radiation pattern with a null in the center. However, different patterns were observed when the phase difference was altered. The phase in one waveguide was altered by changing its width, which increased the phase velocity of the wave propagating inside. The far ends of the two waveguides were connected to a rectangular horn, and the radiation was injected into the atmosphere (Fig. 8). Fig. 7(c) shows the RF radiation distribution produced when the final phase difference was zero. Here, the radiation pattern was solid and had the highest power density achieved, again nearly independent of L.

V. Conclusions

In this paper, we have shown that electromagnetic energy can be transported as surface waves on metallic strips over long distances with high efficiency. Such a transportation system is simple, light, can be easily manufactured, and is only minimally affected by its surroundings. We have also shown that RF can be converted efficiently to surface waves and back, without need of large antennas, enclosed waveguides, or coaxial cables.

References

[1] *Antenna Engineering Handbook*, R. C. Johnson, Ed., McGraw-Hill, New York, 1993.
[2] A. F. Harvey, *Microwave Engineering*. New York: Academic, 1963.
[3] J. A. Stratton, *Electromagnetic Theory*. New York: McGraw-Hill, 1941, p. 527.
[4] G. Goubau, “Surface waves and their applications to transmission lines,” *J. Appl.Phys.*, vol. 21, p. 1119, 1950.
[5] H. F. M. Barlow and A. L. Cullen, “Surface waves,” *Proc. Inst. Elect. Eng.*, vol. 100, pp. 329–427, Nov. 1953.
[6] F. J. Zucker, “Theory and applications of surface waves,” *Nuvo Cimento 9 Sup.*, vol. 3, pp. 450–472, 1952.
[7] W. Rotman, “A study of single-surface corrugated guides,” *Proc. IRE*, vol. 39, pp. 952–959, Aug. 1951.
[8] S. S. Attwood, “Surface-wave propagation over a coated plane conductor,” *J. Appl. Phys.*, vol. 22, pp. 504–509, Apr. 1951.
[9] G. Goubau, “Single-conductor surface-wave transmission lines,” *Proc. IRE*, vol. 39, pp. 619–624, June 1951.
[10] L. J. Chu, “Electromagnetic waves in elliptic hollow pipes of metal,” *J. Appl. Phys.*, vol. 9, pp. 583–591, Sept. 1938.
[11] S. Zhang and J. Jin, *Computation of Special Functions*. New York: Wiley, 1996.
[12] N. W. McLachlan, *Theory and Application of Mathieu Functions*. Oxford, U.K.: Clarenton Press, 1947.

M. Friedman joined the Naval Research Laboratory (NRL), Washington, DC, in February 1971, as a Research Scientist and Consultant to the Plasma Physics Division. He currently is Head of the Advanced Research Section, Laser Plasma Branch. His responsibilities have involved the supervision of the design, conduct, and evaluation of exploratory experiments in the area of pulsed power, generation of intense relativistic electron beams, and their applications.

From 1969 to 1971, he was with Cornell University, where he was involved in the utilization of relativistic electron beams for fusion applications. Prior to joining Cornell University, he was involved with a group on a toroidal turbulent heating experiment (TWIST) at the Culham Laboratory, Abingdon, Berkshire, U.K. From 1960 to 1964, he was with The Weitzman Institute of Science, Rehovof, Israel, during which time he performed doctoral research in cosmic rays and high-energy particles. He has authored or co-authored 11 patents and patent applications and over 80 refereed journal papers.

Dr. Friedman was the recipient of the 1992 Naval Research Laboratory Sigma Xi Applied Science Award.

Richard F. Fernsler received the Ph.D. degree in plasma physics from the University of Maryland at College Park, in 1976.

He was a Post-Doctoral Associate with the National Research Council, Naval Research Laboratory, Washington, DC, until 1977, after which time he joined JAYCOR Inc. Since 1983, he has been with the Naval Research Laboratory. His research has included theoretical investigations of electrical streamers, lightning, glow discharges, laser and microwave breakdown, electron beam propagation, and plasma processing.